ACEEE Int. J. on Electrical and Power Engineering , Vol. 4, No. 3, November 2013

Induction Motors Faults Detection Based on Instantaneous Power Spectrum Analysis with Elimination of the Supply Mains Influence

Mykhaylo Zagirnyak[1], Dmytro Mamchur[2], Andrii Kalinov[3] and Atef S. Al-Mashakbeh[4]
[1, 2, 3] Kremenchuk Mykhailo Ostrohradskyi National University, Kremenchuk 39600 Ukraine
Email: [1]mzagirn@kdu.edu.ua, [2]dm@kdu.edu.ua, [3]scenter@kdu.edu.ua
[4] Electrical Engineering Department, Tafila Technical University
P.O. Box 179, 66110 Tafila – Jordan

***Abstract*—A method of induction motor diagnostics based on the analysis of three-phase instantaneous power spectra has been offered. Its implementation requires recalculation of induction motor voltages, aiming at exclusion from induction motor instantaneous three-phase power signal the component caused by supply mains dissymmetry and unsinusoidality. The recalculation is made according to the motor known electromagnetic parameters, taking into account the electromotive force induced in stator winding by rotor currents. The results of instantaneous power parameters computation proved efficiency of this method in case of supply mains voltage dissymmetry up to 20%. The offered method has been tested by experiments. Its applicability for detection of several stator and rotor winding defects appeared in motor simultaneously has been proved. This method also makes it possible to estimate the extent of defects development according to the size of amplitudes of corresponding harmonics in the spectrum of total three phase power signal.**

***Index Terms*—induction motors, fault diagnosis, instantaneous power, current measurement, voltage measurement, frequency domain analysis, dissymmetry, unsinusoidality, broken bars, MCSA.**

I. Introduction

Induction motors (IM) are most widely used energy consumers and energy converters for different industrial applications. In spite of a very simple and reliable construction, there happen sudden failures of IM, and they may lead to serious faults of the whole work station. This may results in significant pecuniary losses because of repair operations and idle time. Thus, timely diagnostics of incipient IM faults is a very important task. To solve this task the on-line IM diagnostic systems are being developed.

Different reviews [1, 2] showed that most frequently caused IM defects are the following: the bearings defects (32-52%), stator windings defects (15-47%), rotor bars/rings (less than 5%), shaft or coupling defects (about 2%), defects caused by external devices (12-15%), other defects (10-15%). For detection the bearings faults there are well-developed and widely used methods of vibration diagnostics [3]. Thus, this work is devoted to incipient faults detection of stator and rotor. Most common rotor faults are the rotor-to-stator eccentricity and the rotor bar breaks. Most common stator defects are the short circuits in windings and also the windings parametrical asymmetry.

There is a range of methods for incipient fault detection. Widely used are monitoring of mechanical vibrations, currents, reverse sequence pole and partial charges. The aim of these methods is to detect deviations in signal spectra.

Well-known IM incipient faults detection methods are successfully used for large and medium machines. However, there are some limitations to usage of these methods for low-voltage machines because of economical reasons and sensors size.

The analysis of existing IM diagnostic methods gives the following results.

There are a number of methods based on electrical signal spectra analysis, such as Motor Current Signature Analysis (MCSA). They are very popular diagnostic methods because of simplicity of signal recording under operation mode. There are a number of works devoted to using such methods as a medium for detection of stator windings short-circuits, rotor unbalances and rotor bar breaks, and also bearings defects [4–7]. But it has to be mentioned that electrical distortions and influence of the supplying voltage low quality could lead to appearance of harmonics in analyzed electrical signal on the same frequency as a fault harmonics. This may lead to wrong diagnosis. To eliminate such shortcomings of these methods, the additional analysis by vibrations [4] or more complicated mathematical apparatus for analysis [5–7] are used. However, even this additional analysis does not prevent diagnostic mistakes when low-power IMs with significant influence of voltage unsinusoidality are under analysis. This fact is especially significant for IM fed from low-voltage supply of industrial plants.

Another well-known diagnostic method is supply voltage analysis [8–10]. The data are analyzed either according to supply voltage spectra with neutral voltage [9], or high frequency carrying signal [10]. As for the first mentioned method, diagnostic result significantly depends on voltage quality, which is not always ideal in low-voltage supply mains with IM. As for the second mentioned method, there is necessity of using additional equipment for generation test carrying signals.

Also there is a range of methods for fault detections under transient conditions. But these methods provides the best results for analysis in starting, braking modes, and modes

DOI: 01.IJEPE.4.3.5

under transient load, when there are significant signal changes both in time and frequency domains. Thus, these methods are less convenient for steady state modes analysis.The instantaneous power spectra analysis allows avoiding shortcomings of above mentioned methods [11, 12]. Instantaneous power spectra analysis allows both detection of fault presence and estimation of damage level by analysis of proper harmonic value. Thus, instantaneous power spectra analysis allows one to estimate the energy of fault and the correlation of this energy to additional damage of IM parts under influence of additional vibrations caused by proper harmonic. Moreover, the instantaneous power spectra analysis allows analyzing of IM operation modes under significant nonlinearity, when it is incorrect to use superposition principle for current harmonics. Also, instantaneous power analysis is more reliable, it is less dependent on noise, and gives additional harmonic components for analysis [11, 12].

In [13] it was offered to monitoring and estimation of IM operating conditions by means of instantaneous power and electromagnetic torque spectra analysis. As it was mentioned, it is very important to take into account supply voltage quality for making proper diagnosis of low-power IM. A number of authors have investigated the influence of supplying voltage low-quality on parameters and operation modes of low-power IM [14]. It leads to conclusion that it is necessary to eliminate the influence of noises, asymmetry and non-sinusoidality of supply voltage on analyzed currents and power signals. It improves accuracy and reliability of diagnostic.

II. Problem Statement

The method of IM diagnostic based on 3-phase IM power spectra analysis is offered. To achieve accuracy and reliability of diagnostic results it is necessary to eliminate the influence of power spectra components caused by supply voltage low quality on components caused by IM defects.

III. Research Method

IM diagnostics basing on 3-phase motor instantaneous power spectra analysis is carried out on the basis of measured stator currents and voltages. In case of voltage supply low-quality, both the motor non-linear elements and the network non-sinusoidality and dissymmetry cause harmonics in current signal spectra. Thus, IM diagnostic based on MCSA may lead to wrong result. It is possible to increase reliability of diagnostic methods based on current and power spectra analysis by means of elimination the influence of supply voltage low-quality and non-sinusoidality on analyzed signals. To eliminate the influence of supply voltage low quality and to provide possibility of current and power signals analysis as signals, given from sinusoidal symmetric supply, it is necessary to recalculate current and power harmonics values taking into account linear dependence of complex impedances $\dot{Z}_k$ on their sequence number according to a well-known expression (Fig. 1):

$$\dot{Z}_k = Re[Z] + j\, Im[Z]k,$$

which can be reduced for the higher harmonics to the following form:

$$\dot{Z}_k = 2(R_1 + R_2) + 2j(L_1 + L_2)\omega_k,$$

in this case, for IM, computed dependence of complex impedance harmonics amplitude values module on harmonic number presents a straight line (Fig.1).

Harmonics recalculation is made in a complex form. It is correct if IM is presented as a linear and nonlinear objects totality. Then, the superposition principle is observed if the current harmonics of linear object part, which are caused by the presence of the mains voltage higher harmonics, are determined by means of dividing them by motor complex impedance. IM complex impedance can be determined as a result of electromagnetic parameters identification process. The main nonlinearity in this condition is determined by the effect of current displacement in rotor windings, if the absence of IM magnetic system saturation in the short-circuit duty is taken into consideration. Current displacement effect is significantly manifested at frequencies above 250 Hz. In this case, the data obtained in the short-circuit duty correlate to the data received for idle running condition with polyharmonic supply. There are considerable differences in the first harmonic amplitudes where rotation electromotive force (EMF), which is induced in stator winding, has great influence (Fig.1). The difference of higher frequencies harmonics can be explained by the influence of magnetic system saturation and the presence of small value of above mentioned EMF which constitutes the motor complex nonlinearity.

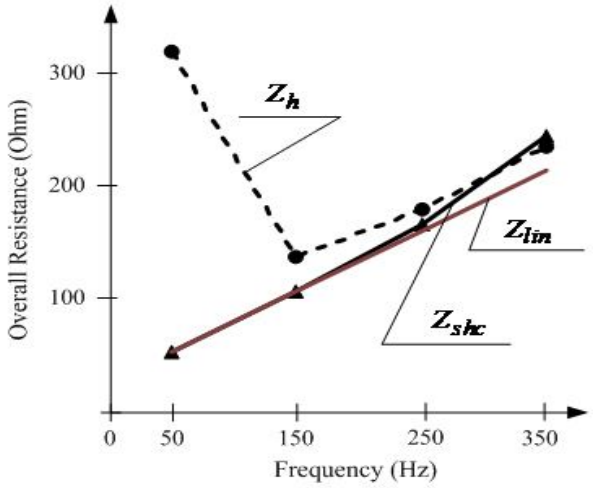

Fig.1. Deviation of complex impedances (Z_{lin}) dependences on higher harmonics number in the short-circuit duty (Z_{shc}) and an idle running (Z_h).

To analyze the influence of supply low-quality parameters on the results of IM diagnostics, a number of experiments were done with artificial creation of supply voltage dissymmetry for induction motor type AO 90 S-4 (1.1 kW; 1410 rpm; 2.8 A). Dissymmetry was created by means of connecting an autotransformer to an IM phase. Characteristics of voltage parameters for the most typical experiments are shown in Table I.

DOI: 01.IJEPE.4.3.5

TABLE I. VOLTAGE PARAMETERS IN EXPERIMENTS WITH ARTIFICIALLY CREATED SUPPLY DISSYMMETRY

Experiment number	ε_2 , %	KU , %
1	0.7	0.9
2	20.09	16
3	58.8	69

The following designations are adopted in Table I: KU is voltage deviation in autotransformer phase; ε_2 is reverse sequence coefficient computed according to the following expression:

$$\varepsilon_2 = U_2 / U_r , \quad (1)$$

where U_2 is a reverse sequence voltage, U_r is a rated voltage.

Voltage deviation is computed according to the following expression:

$$KU = \frac{U_A - U_r}{U_r} 100\% , \quad (2)$$

where U_A is a phase voltage effective value, U_r is a rated phase voltage.

The analysis of three-phase IM operation conditions depends on the presence or absence of the connection between zero points of mains and IM. Often, IM stator winding zero point is not brought out into the junction box, and is not connected to zero wire of the supply mains.

EMF induced in IM stator winding by rotor currents significantly influences formation of currents in stator phases. When ohmic resistance and stator winding leakage inductance are known, this EMF is computed according to expression (for phase A):

$$e_A(t) = u_A(t) - i_A(t) R_{1A} - L_{1A} \frac{di(t)}{dt} , \quad (3)$$

where $u_A(t)$, $i_A(t)$ are instantaneous values of voltages and currents of the phase, correspondingly; t is a time; R_{1A}, L_{1A} are ohmic resistance and leakage inductance of the stator phase winding.

When there is dissymmetry in the supply mains, the stator phase currents and voltages dissymmetry occurs in IM. In this case, due to rotor revolutions EMF, stator phase voltages dissymmetry considerably differs from the supply mains voltages dissymmetry and is additionally manifested in dissymmetry about abscissa axis (time axis). Experimental curves for supply mains voltages and motor voltages and currents for experiment No. 3 (Table I) are shown in Fig. 2.

Analysis of dissymmetry level in three-phase system without connections of mains and induction motor neutral terminals according to currents and voltages phase values is rather difficult. That is why this analysis should be carried out on the basis of interphase parameters:

$$u_{AB}(t) = u_A(t) - u_B(t); \quad u_{BC}(t) = u_B(t) - u_C(t); \quad u_{CA}(t) = u_C(t) - u_A(t). \quad (4)$$

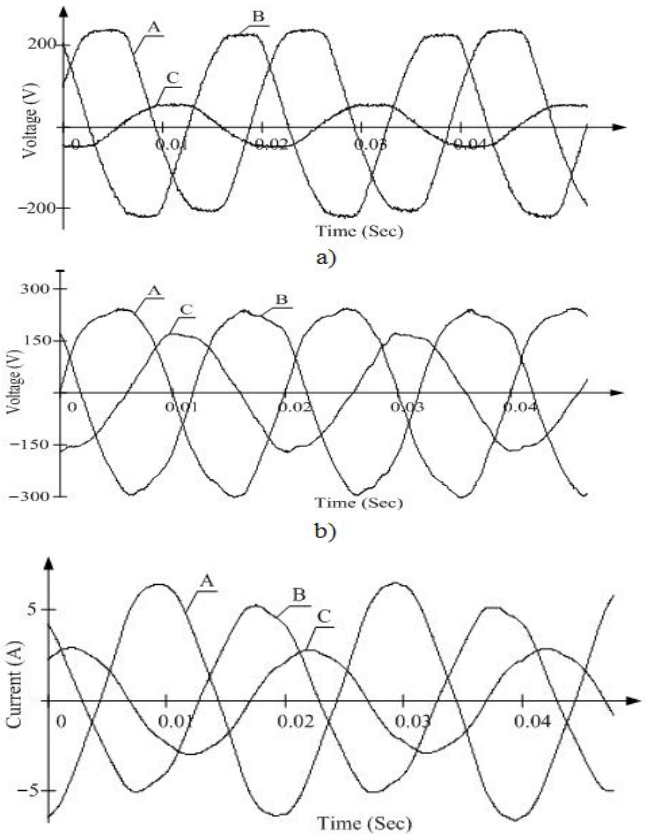

Fig.2. Supply mains phase voltages (a) and IM phase voltages (b) and currents (c) for experiment No. 3.

Then three-phase IM instantaneous power can be expressed through interphase parameters, which makes it possible to recalculate the instantaneous power value without using phase values:

$$p(t) = 1/3\left(\left(i_A(t) - i_B(t)\right)u_{AB}(t) + \left(i_B(t) - i_C(t)\right)u_{BC}(t) + \left(i_C(t) - i_A(t)\right)u_{CA}(t)\right). \quad (5)$$

Interphase currents and voltages do not have dissymmetry about abscissa axis (Fig. 3), as they do not contain zero sequence components.

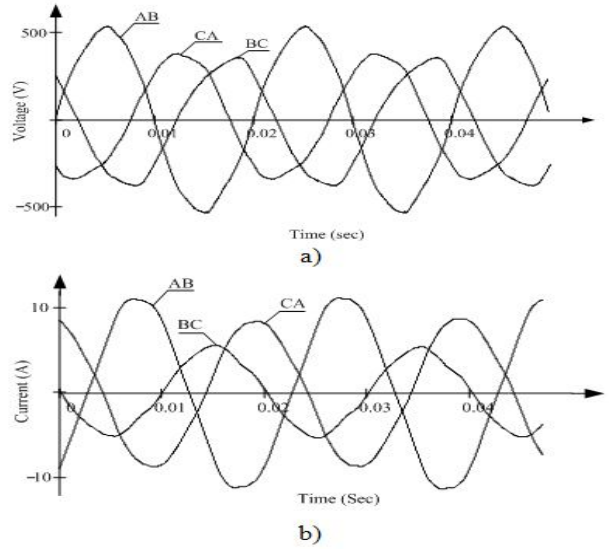

Fig.3. IM interphase voltages (a) and currents (b) for experiment No.3.

DOI: 01.IJEPE.4.3.5

Then recalculation of current harmonics is made according to expression:

$$\dot{I}'_{k_{AB}} = \dot{I}_{k_{AB}} - \frac{\dot{U}_{k_{AB}}}{\dot{Z}_{k_{AB}}}, \quad (6)$$

where $\dot{I}_{k_{AB}} = \left(\dot{I}_{k_A} - \dot{I}_{k_B}\right)$ is the complex value of current k-th harmonic, $\dot{U}_{k_{AB}}$ is the complex value of interphase voltage k-th harmonic, $\dot{Z}_{k_{AB}}$ is the IM complex impedance value on k-th harmonic, $k=2..K$ is harmonic number.

During recalculation of the current phase fundamental harmonic it is necessary to take into account EMF induced in stator winding:

$$\dot{I}''_1 = \dot{I}_1 - \frac{\dot{U}_1 - \dot{E}_1}{\dot{Z}_1}, \quad (7)$$

where $\dot{E}_1$ is the complex value of EMF first harmonic amplitude in the gap; $\dot{Z}_1 = R_1 + jL_1\omega$ is the complex value of impedance first harmonic. Recalculation of currents instantaneous values is made according to (6):

$$\begin{aligned} i'_{AB}(t) &= 2\sum_{k=2} Re\left(I'_{k(AB)}\right)cos(k\omega t) - \\ &- 2\sum_{k=2} Im\left(I'_{k(AB)}\right)sin(k\omega t) + \\ &+ 2\left(Re\left(I''_{1(AB)}\right)cos(\omega t) - Im\left(I''_{1(AB)}\right)sin(\omega t)\right), \end{aligned} \quad (8)$$

voltage is assigned by the first harmonic:

$$\begin{aligned} u'_{AB}(t) &= 2\sum Re\left(U_{1(AB)}\right)cos(\omega t) - \\ &- 2\sum Im\left(U_{1(AB)}\right)sin(\omega t), \end{aligned} \quad (9)$$

where $i'_{AB}(t)$ are recalculated current instantaneous values according to (5), $u'_{AB}(t)$ are supply ideal voltages without higher harmonics, ω is an angular frequency. Recalculation for currents $i'_{BC}(t)$, $i'_{CA}(t)$ and voltages $u'_{BC}(t)$, $u'_{CA}(t)$ is carried out similarly to expressions (8) and (9), correspondingly.

The influence of supply mains dissymmetry on current signals formation can be eliminated by restoration of voltage signals basing on the first harmonics of stator phase voltages, according to (9). Interphase voltage is taken as a basic signal because it least of all differs from rated voltage. Instantaneous values of other interphase voltages are computed in relation to the basic one from three-phase mains symmetry condition:

$$\dot{U}_{1(BC)} = \dot{U}_{1(AB)} e^{\frac{-j2\pi}{3}};$$

$$\dot{U}_{1(CA)} = \dot{U}_{1(AB)} e^{\frac{-j4\pi}{3}},$$

where $\dot{U}_{1(AB)}$, $\dot{U}_{1(BC)}$, $\dot{U}_{1(CA)}$ are complex values of the first harmonics of interphase voltages AB, BC and CA, correspondingly.

Then, according to (7), current harmonics are recalculated. It should be mentioned that it is not necessary to recalculate EMF harmonics when supply mains dissymmetry is less then 20%, as there is no significant magnetic field distortion in IM gap. Experimental data for different levels of supply mains dissymmetry, showed the following results. When there is conditional supply mains symmetry (experiment No.1), EMF dissymmetry computed similarly to (2), is $KE = 0.27\%$ (Fig. 4). When supply mains are dissymmetrical as for experiment No. 2, EMF dissymmetry is $KE = 2.9\%$ (Fig.5), and when supply mains are dissymmetrical as for experiment No. 3, EMF dissymmetry is $KU = 15.1\%$ (Fig.6).

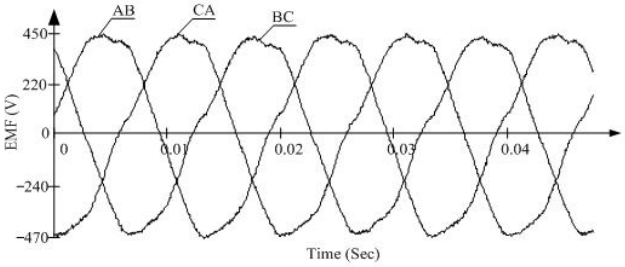

Fig. 4. Interphase EMF in the gap for experiment No. 1

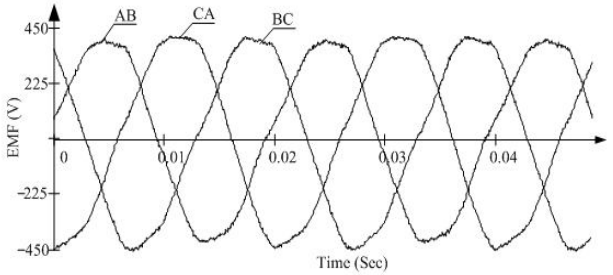

Fig. 5. Interphase EMF in the gap for experiment No. 2

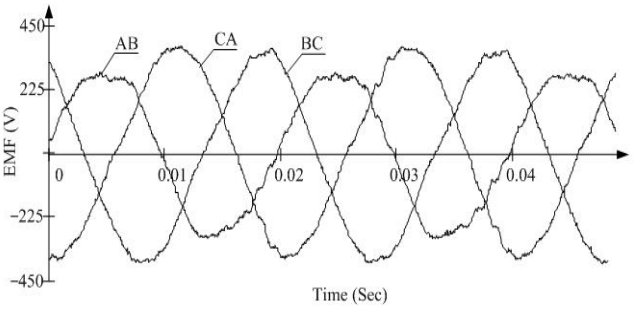

Fig. 6. Interphase EMF in the gap for experiment No. 3

IV. Experimental Verification

To research the efficiency of the offered method application, let us analyze signal experimental data for the mentioned (Table I) experiments.

Using methods of IM parameters identification, stator and rotor ohmic resistance and inductive reactance, which are necessary for the further analysis, were preliminary computed for analyzed IM AO 90 S-4 (*1.1* kW; *1410* rpm; *2.8* A):

DOI: 01.IJEPE.4.3.5

$R_1 = 7.62$ Ohm , $R_2 = 8.06$ Ohm , $L_1 = 0.02239$ H , $L_2 = 0.02057$ H.

After recalculation of experimental signals according to expressions (6–8), currents and voltage signals for the further analysis are obtained (Fig.7).

Three-phase instantaneous power values are computed on the basis of recalculated interphase currents and voltages (Figs. 8–10).

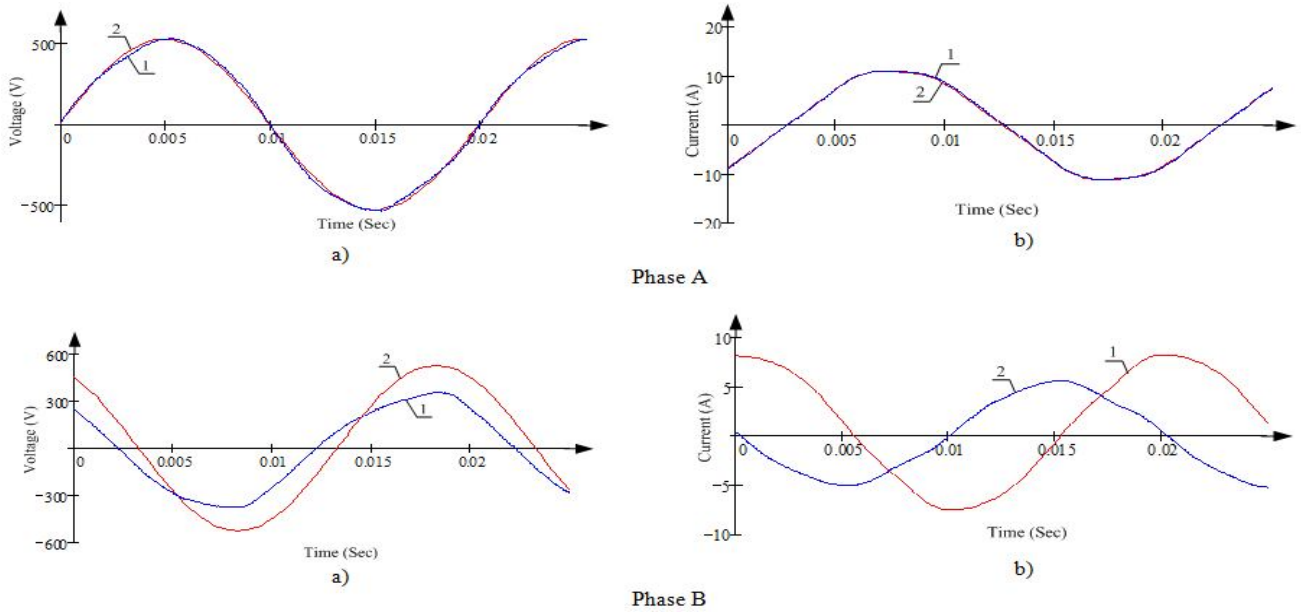

Fig.7. Signals of initial (1) and recalculated (2) voltages (a) and currents (b) obtained for experiment No. 3 (begining).

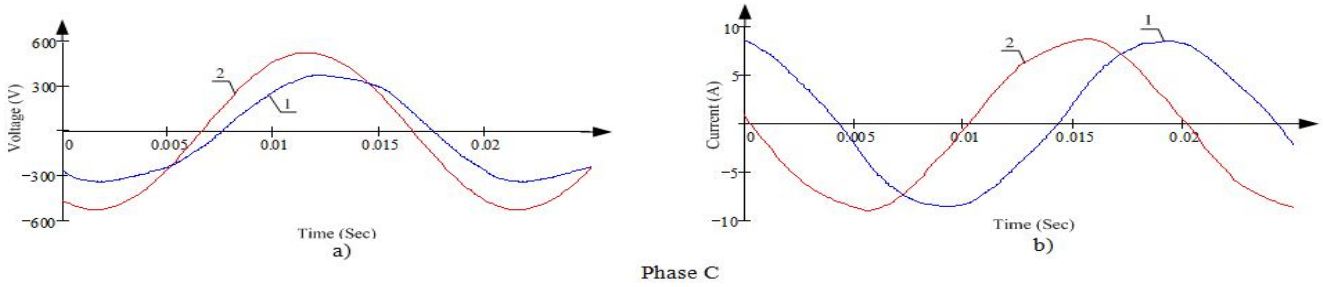

Fig.7. Signals of initial (1) and recalculated (2) voltages (a) and currents (b) obtained for experiment No. 3 (ending).

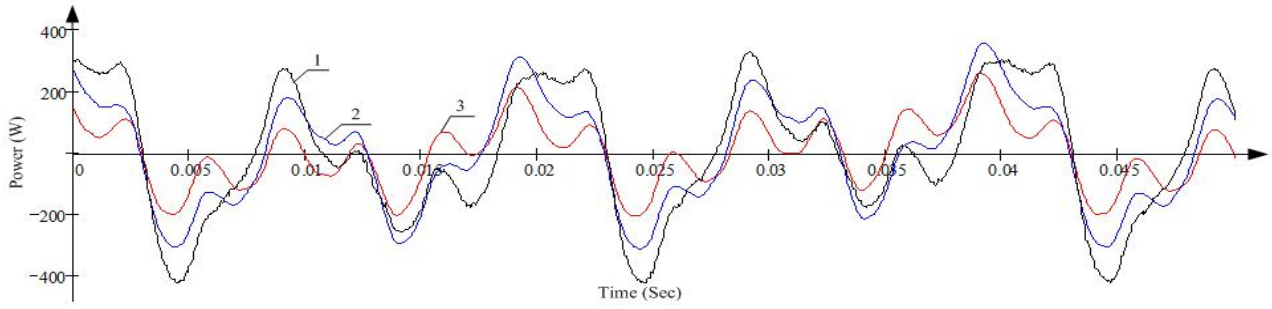

Fig.8. Total three-phase power without taking constant component into account for experiment No. 1.

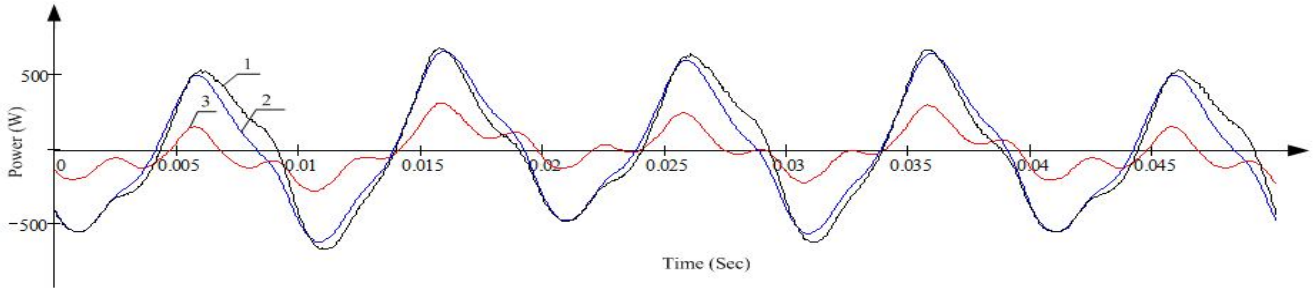

Fig.9. Total three-phase power without taking constant component into account for experiment No. 2.

DOI: 01.IJEPE.4.3.5

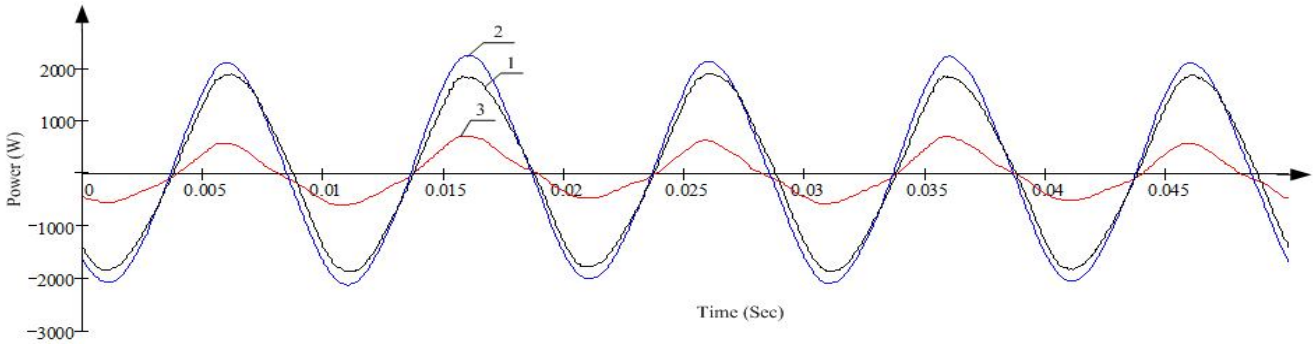

Fig.10. Total three-phase power without taking constant component into account for experiment No. 3.

The following designations are adopted in Figs. 8-10: 1 is an initial signal, 2 is a signal transformed to sinusoid supply, 3 is a signal transformed to sinusoidal symmetric supply.

Obvious difference of initial and restored signals can be observed using spectral analysis (Figs 11-13). The following designations are adopted in Figs. 11-13:

× is initial signal, P_{init} ; △ is signal after elimination of the influence of supply mains unsinusoidality, P_{asym} ; ○ is signal after elimination of the influence of supply mains unsinusoidality and dissymmetry, P_{sym} .

For comparative analysis of initial and the recalculated signals, dissymmetry coefficients, and also currents and voltages unsinusoidality were calculated, as well as power higher harmonics coefficient K_{Phg} (10), the computation of which was made according to the following expression:

$$K_{Phg} = \sqrt{\sum_{v=1}^{N-1} P_v^2} \Big/ P_r \ . \qquad (10)$$

As it can be seen from (12), the offered coefficient is a relation of power higher harmonics root-mean-square value to motor power P_r rated value.

The results of computation of the mentioned coefficients are given in Tables II-IV.

The analysis of the data (Tables III, IV) for elimination of low-quality supply mains parameters influence, showed following results. Currents signals assume a larger degree of dissymmetry and unsinusoidality, i.e. harmonics occurring due to motor faults are manifested in current signal spectrum more evidently. In this case, a number of harmonics, caused by low-quality supply mains, disappear (Figs 11-13). For all the experiments, a number of total instantaneous power harmonics with frequencies 150, 250, 350 Hz, caused by supply mains interharmonics, are eliminated. As it can be seen from Table II, power higher harmonics coefficient reduces, when dissymmetry level is about 20%. It decreases to the level which could be observed when supply is provided by symmetrical mains.

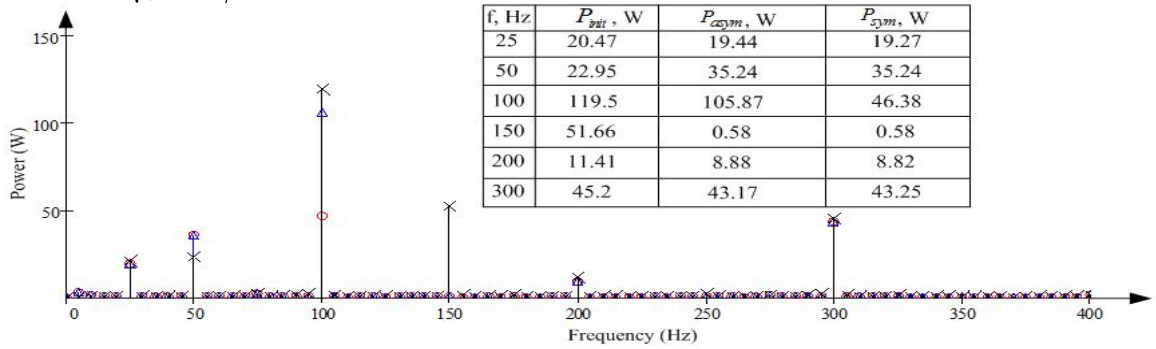

f, Hz	P_{init} , W	P_{asym}, W	P_{sym}, W
25	20.47	19.44	19.27
50	22.95	35.24	35.24
100	119.5	105.87	46.38
150	51.66	0.58	0.58
200	11.41	8.88	8.82
300	45.2	43.17	43.25

Fig. 11. Spectral composition of total three-phase instantaneous power for experiment No. 1.

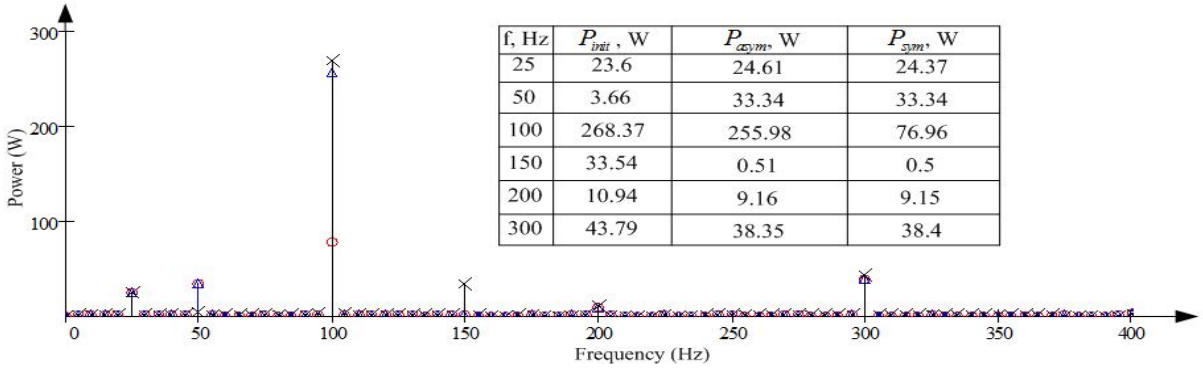

f, Hz	P_{init} , W	P_{asym}, W	P_{sym}, W
25	23.6	24.61	24.37
50	3.66	33.34	33.34
100	268.37	255.98	76.96
150	33.54	0.51	0.5
200	10.94	9.16	9.15
300	43.79	38.35	38.4

Fig. 12. Spectral composition of total three-phase instantaneous power for experiment No. 2.

DOI: 01.IJEPE.4.3.5

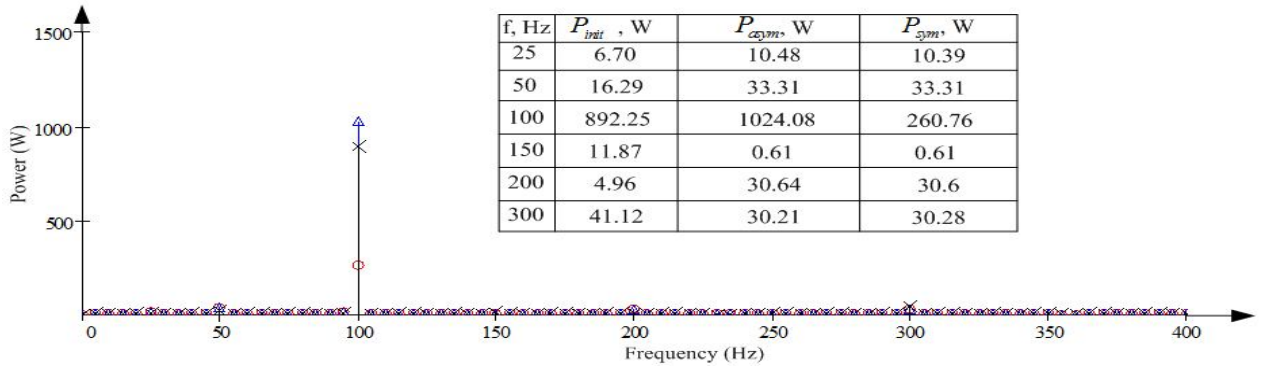

f, Hz	P_{init} , W	P_{asym}, W	P_{sym}, W
25	6.70	10.48	10.39
50	16.29	33.31	33.31
100	892.25	1024.08	260.76
150	11.87	0.61	0.61
200	4.96	30.64	30.6
300	41.12	30.21	30.28

Fig. 13. Spectral composition of total three-phase instantaneous power for experiment No. 3.

TABLE II. COMPUTED VALUES OF POWER HIGHER HARMONICS COEFFICIENTS

No.	Type of the analyzed signal	Value K_{Phg}		
		Experiment number		
		1	2	3
1	Transformed to supply by symmetric sinusoid mains	0.069	0.087	0.243
2	Transformed to supply by dissymmetric sinusoid mains	0.111	0.238	0.933
3	Initial signal	0.129	0.250	0.812

TABLE III. COMPUTED VALUES OF ANALYZED SIGNALS UNSINUSOIDALITY COEFFICIENTS

No.	Parameter		Initial signal			Restored signal		
			Experiment number			Experiment number		
			1	2	3	1	2	3
1	Current	I_{AB}	5.72 %	5.18 %	2.9 %	5.98 %	5.28 %	2.85 %
		I_{BC}	5.38 %	11.4 %	6.67 %	6.16 %	6.67 %	4.09 %
		I_{CA}	5.61 %	5.83 %	4.44 %	5.7 %	5.33 %	4.18 %
2	Voltage	U_{AB}	6.28 %	5.56 %	4.42 %	0 %	0 %	0 %
		U_{BC}	6.17 %	5.95 %	7.34 %	0 %	0 %	0 %
		U_{CA}	6.32 %	6.15 %	6.71 %	0 %	0 %	0 %

TABLE IV. COMPUTED VALUES OF ANALYZED SIGNALS DISSYMMETRY COEFFICIENTS

No.	Parameter	Initial signal			Restored signal		
		Experiment number			Experiment number		
		1	2	3	1	2	3
1	Current	30.4 %	72.45 %	283.58 %	13.88 %	23.65 %	76.69 %
2	Voltage	3.88 %	10.71 %	45.54 %	0 %	0 %	0 %
3	Power	23.44 %	20.45 %	10.44 %	0.06 %	0.44 %	0.14 %

According to these data, it is possible to make the conclusion about presence of IM faults, using indicators formulated in paper [13].

The tested motor used in the experimental investigation was a three-phase induction machine type AO 90 S-4, 50 Hz, 4-pole, 1.1 kW, 1410 rpm; 2.8 A. For investigation of turn-to-turn short circuit in stator windings, the taps were provided in one of the stator winding phases to imitate turn-to-turn short circuits (Fig. 14, Table V).

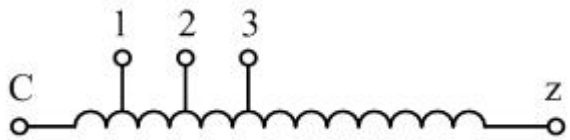

Fig. 14. Stator phase winding taps circuit.

For broken bars investigation several rotors of identical type with 1, 2, 3 or 4 broken bars, which can be interchanged, were used (Fig. 15). DC generator provided a mechanical load.

TABLE V. IM WINDING RESISTANCE MEASUREMENT DATA

Phase	Resistance value, ohm		
A	7.576		
B	7.632		
C	7.66		
Taps in phase C	Winding part	Resistance value, ohm	Reduction of winding turns number, %
	1-z	7.45	2.74
	2-z	6.9	10
	3-z	6.31	17.6

DOI: 01.IJEPE.4.3.5

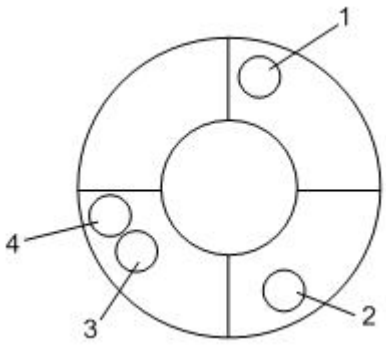

Fig. 15. Scheme of rotor apertures location:
1, 2, 3, 4 are broken bar numbers.

Correspondence of the existing faults to the fulfilled experiments sequence number is shown in Table VI.

TABLE VI. EXPERIMENTS WITH IM ARTIFICIAL DAMAGES

No.	Fault type
1	IM basic variant without artificial defects
2	IM with a screwed-out bolt No.1
3	IM with a screwed-out bolt No.1 and phase C winding short circuit 2.74%
4	IM with a screwed-out bolt No. 1 and phase C winding short circuit 10%
5	IM with a screwed-out bolt No. 1 and phase C winding short circuit 17.6 %
6	IM with screwed-out bolts No. 1 and No. 2
7	IM with screwed-out bolts No. 1, No.2 and No.3
8	IM with screwed-out bolts No. 1, No.2, No. 3 and No.4

A measuring module and software were developed by authors [14] for measurement and record of electrical values (voltages and currents) necessary for the analysis (Fig. 16).

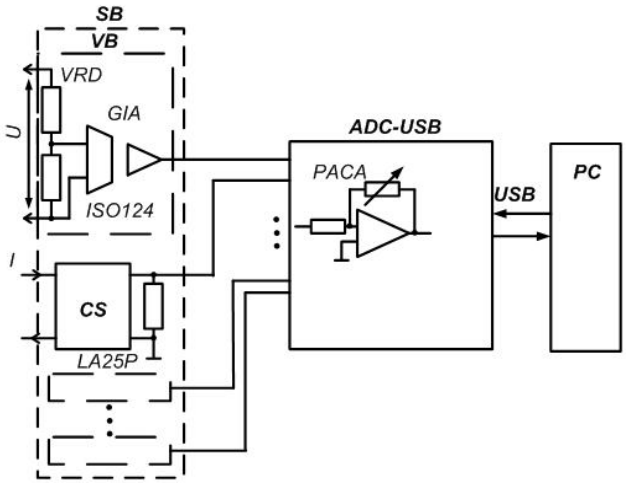

Fig. 16. Measuring module functional circuit:
SB – sensor block; VB – voltage block; VRD – voltage resistance divider; GIA – galvanic isolation amplifier;
CS – current sensor; PC – personal computer; PACA – programmed amplification coefficient amplifier; USB – PC bus.

The following assumptions were accepted for experimental researches. The possibility of load variation was not taken into account. This variation may lead to appearance of interharmonics and low-frequency harmonics in power spectra. Interharmonics do not make significant influence on informative harmonics which are used for analysis. The influence of low-frequency harmonics could be compensated by analysis of three-phase IM instantaneous power mean value. The influence of heating appears in changes of windings active resistances. In case of uniform heating the active resistances will change symmetrically. Nonuniform heating mainly leads to clearer asymmetry demonstration. It could be observed by difference between amplitude harmonics by phases. Researches [13] showed that the main influence of saturation appears on 6-th and its multiple harmonics of instantaneous power. However, harmonics of lower frequencies were used in this work. It has to be mentioned, that offered method could be used both for variable speed motor and for fixed speed motor based on voltage inverter (with PWM).

Analysis was carried out for IM idle conditions and for half load conditions. Preliminary data analysis showed that defects could be more obviously manifested in loaded machine signals. Thus, following analysis is presented for half loaded conditions. Experimental data analysis leads to conclusion that elimination of supply voltage unsinusoidality and dissymmetry allows removing from consideration harmonics caused by voltage low-quality. This simplifies the analysis and improves diagnostics results (Fig. 17-20).

Experimental data analysis showed, that the following defects were present in the basic variant of motor without artificial demages (experiment No. 1, Table VI):

– rotation speed harmonics (24.8 Hz for tested IM) and its multiple in current and power spectra shows misalignment of shaft and actuator (Fig. 17);

– double supply frequency in three-phase power spectra (100 Hz) shows base motor dissymmetry. Its low value confirms good motor condition;

– power harmonic multiple of six supply main harmonic shows IM nonlinearity and influence of magnetizing curve;

– power harmonic multiple of for supply main harmonic shows presence of both motor nonlinearity and dissymmetry and appears as result of multiplying of proper current and voltage harmonics.

The values of considered harmonics for base IM are not significant. These values are less then 2% of rated power. It shows motor good conditions.

Experimental data analysis for rotor with one broken bar (experiment 2, Table VI) leads to the following conclusions.

Two sideband components appear around fundamental component at following frequencies

$$f_{bb} = f_n(1 \pm ns)$$

where f_n is a fundamental frequency, s is a motor slip, $n = 1,2,...$

When supply mains low-quality influence on current signal is eliminated, sideband components became more clearly visible (Fig. 17b, 19b).

Three-phase power spectra, in addition to two sideband components around double fundamental component, contain component at the modulation frequency (Fig. 18, 20). This component provides additional diagnostic information about

DOI: 01.IJEPE.4.3. 5

motor conditions, and allows improving reliability and accuracy of diagnostics [11, 12].

When turn-to-turn short circuits appear, as well as when there is stator windings asymmetry, the amplitude of harmonics of the frequency of 100 Hz increases significantly. Separation of these defects is possible when power coefficient $\cos\varphi$ is calculated, as in the presence of turn-to-turn short circuits, unlike asymmetry of stator windings, the angle of current and voltage phase shear reduces, i.e. the value of this coefficient increases (Table VII, experiments 4, 5).

TABLE VII. ANALYSIS OF EXPERIMENTS WITH IM ARTIFICIAL DAMAGES

Experiment No. according to Table VI	$cos(\varphi)$	K_{Phg}
1	0.16	0.054
2	0.14	0.088
3	0.19	0.0825
4	0.39	0.216
5	0.53	0.444
6	0.176	0.0915
7	0.16	0.1115
8	0.15	0.1185

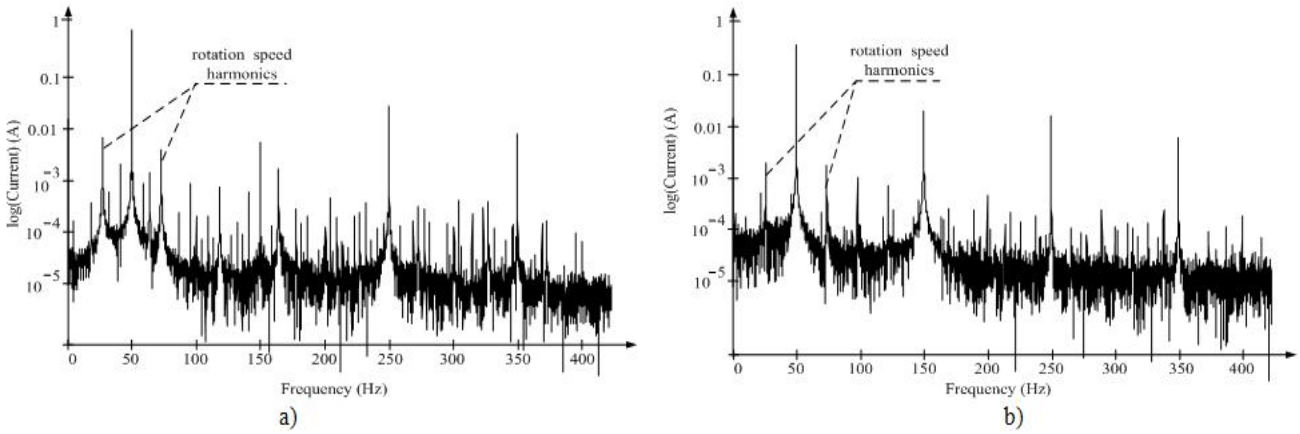

Fig. 17. Current spectra for experiment No.1: base signal (a) and signal after supply low-quality elimination (b)

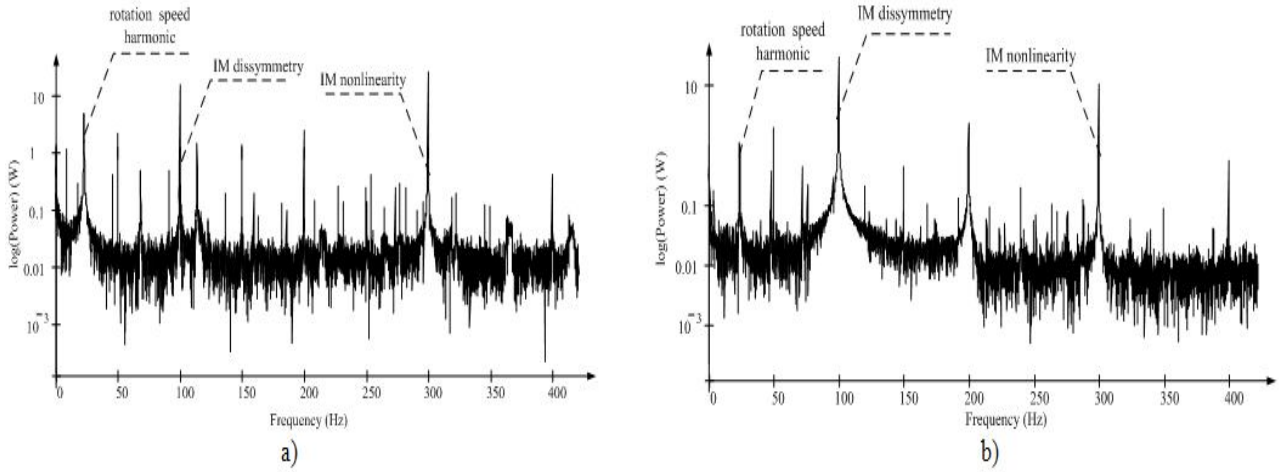

Fig. 18. 3-phase power spectra for experiment No.1: base signal (a) and signal after supply low-quality elimination (b)

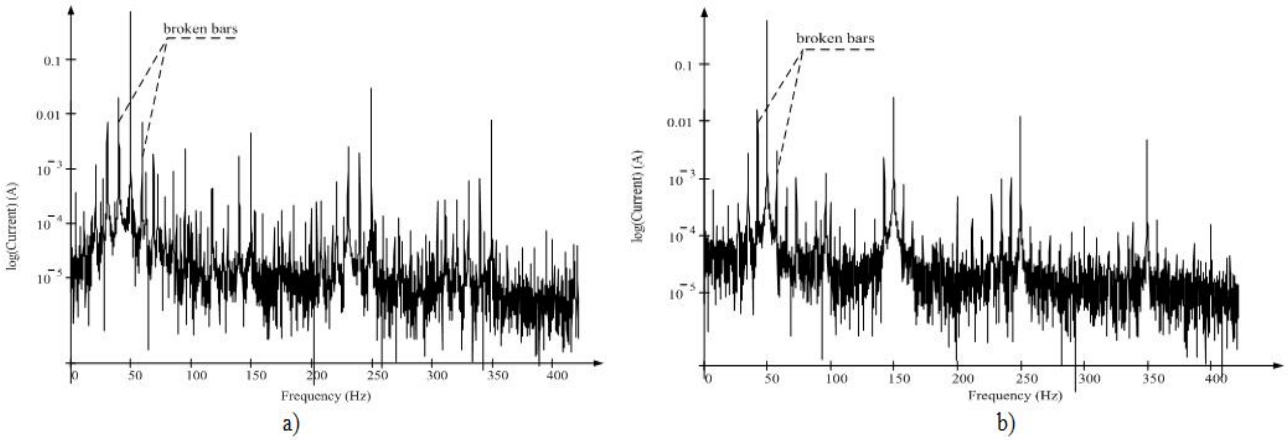

Fig. 19. Current spectra for experiment No.2: base signal (a) and signal after supply low-quality elimination (b)

DOI: 01.IJEPE.4.3.5

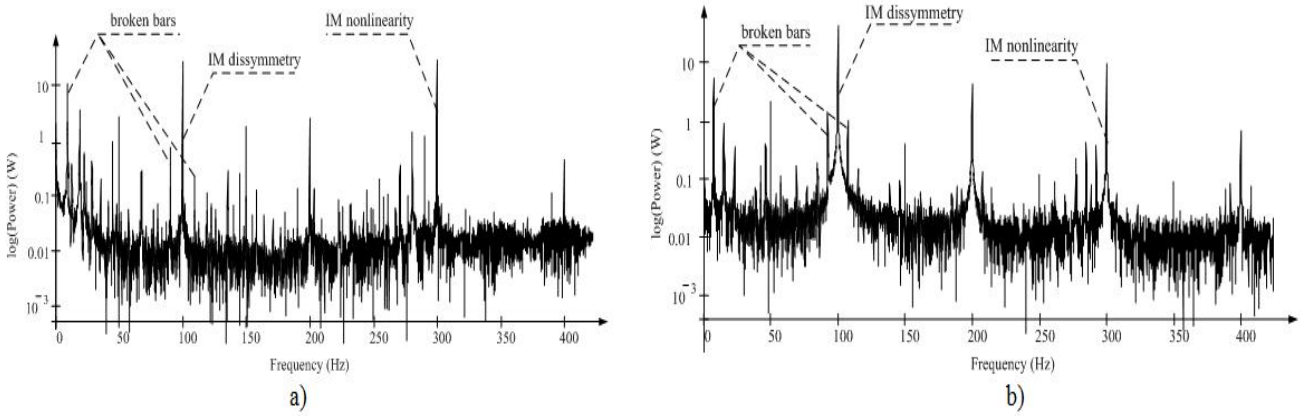

Fig. 20. Three-phase power spectra for experiment No.2: base signal (a) and signal after supply low-quality elimination (b)

Thus, experimental verification of IM diagnostic method based on instantaneous power spectra analysis showed its utility for rotor bar breaks and stator windings short-circuits detection. The diagnostics simplification and improvement due to elimination of supply voltage low-quality, was confirmed.

This method was successfully implemented in Induction motor diagnostic system based on power spectra analysis [15].

V. Conclusions

An IM diagnostic method, based on three-phase instantaneous power spectra analysis, was considered. To improve reliability of diagnostic results by means of supply voltage low-quality elimination, a method for recalculation of stator interphase voltage and current harmonic components was developed and experimentally tested. This method makes it possible to analyze the spectrum of consumed three-phase instantaneous power without components caused by supply mains low-quality parameters. This method provides improved accuracy and information value of IM diagnostics on the basis of the analysis of the spectrum of consumed three-phase instantaneous power.

The method of IM diagnostics on the basis of the analysis of three-phase instantaneous power has been checked experimentally and its applicability to determination of stator and rotor winding several defects simultaneously has been proved. The possibility of estimation of the extent of defects development according to the value of the amplitude of consumed power correspondent harmonic has been shown.

References

[1] O. V. Thorsen and M. Dalva, “A survey of faults on induction motors in offshore oil industry, petrochemical industry, gas terminals, and oil refineries”, IEEE Transactions on Industry Applications, vol. 31, no. 5, pp. 1186–1196, Sep./Oct. 1995.

[2] M. E. H. Benbouzid and G. B. Kliman, “What stator current processing-based technique to use for induction motor rotor faults diagnosis?”, IEEE Transactions on Energy Conversion, vol. 18, no. 2, pp. 238–244, Jun. 2003.

[3] I. Y. Onel, K. B. Dalci and I. Senol, “Detection of outer raceway bearing defects in small induction motors using stator current analysis”, Sadhana, vol. 30, no. 6, pp. 713–722, Dec. 2005.

[4] C. Concari, G. Franceschini and C. Tassoni, “Differential Diagnosis Based on Multivariable Monitoring to Assess Induction Machine Rotor Conditions”, IEEE Transactions on Industrial Electronics, vol. 55, no. 12, pp. 4156–4166, Dec. 2008.

[5] A. Bellini, A. Yazidi, F. Filippetti, C. Rossi and G.-A. Capolino, “High Frequency Resolution Techniques for Rotor Fault Detection of Induction Machines”, IEEE Transactions on Industrial Electronics, vol. 55, no. 12, pp. 4200–4209, Dec. 2008.

[6] M. Blodt, D. Bonacci, J. Regnier, M. Chabert and J. Faucher, “On-Line Monitoring of Mechanical Faults in Variable-Speed Induction Motor Drives Using the Wigner Distribution”, IEEE Transactions on Industrial Electronics, vol. 55, no. 2, pp. 522–533, Feb. 2008.

[7] J. Cusido, L.Romeral, J.A. Ortega, J.A. Rosero and A. Garcia Espinosa, “Fault Detection in Induction Machines Using Power Spectral Density in Wavelet Decomposition”, IEEE Transactions on Industrial Electronics, vol. 55, no. 2, pp. 633–643, Feb. 2008.

[8] M. Nemec, K. Drobnic, D. Nedeljkovic, R. Fiser and V. Ambrozic, “Detection of Broken Bars in Induction Motor Through the Analysis of Supply Voltage Modulation”, IEEE Transactions on Industrial Electronics, vol. 57, no. 8, pp. 2879–2888, Aug. 2010.

[9] A. Khezzar, M. El Kamel Oumaamar, M. Hadjami, M. Boucherma and H. Razik, “Induction Motor Diagnosis Using Line Neutral Voltage Signatures”, IEEE Transactions on Industrial Electronics, vol. 56, no. 11, pp. 4581–4591, Nov. 2009.

[10] F. Briz, M.W. Degner, P. Garcia and A.B. Diez, “High-Frequency Carrier-Signal Voltage Selection for Stator Winding Fault Diagnosis in Inverter-Fed AC Machines”, IEEE Transactions on Industrial Electronics, vol. 55, no. 12, pp. 4181–4190, Dec. 2008.

[11] S.F. Legowski, A.H.M. Sadrul Ula and A.M. Trzynadlowski, “Instantaneous power as a medium for the signature analysis of induction motors”, IEEE Transactions on Industrial Electronics, vol. 32, no. 4, pp. 904–909, Jul./Aug. 1996.

[12] Wang Li, Wang Xuan and Wei Min, “Motor Bearing Fault Diagnosis Based on Wavelet Packet Decomposition of Instantaneous Power”, in Proc. of International Conference on Computer Design and Applications (ICCDA), 2010, vol. 3, pp. V3-457-–-V3-459.

[13] Dmytro Mamchur, Andriy Kalinov “Diagnostics of Asynchronous Motors Based on Spectra Analysis of Power Consumption,” in Proc. XI International Ph Workshop

DOI: 01.IJEPE.4.3.5

OWD'2009, Poland, Gliwice, 2009, pp. 434-439. Available: http:/ /mechatronika.polsl.pl/owd/pdf2009/434.pdf

[14] M. V. Zagirnyak, D. G. Mamchur and A. P. Kalinov, "The theory and application of the induction motor diagnostic methods based on electrical signal analysis," Journal of Energy Technology (JET), Vol. 5, Iss. 2, pp. 37–50, May 2012.

[15] M. V. Zagirnyak, D. G. Mamchur and A. P. Kalinov, "Comparison of induction motor diagnostic methods based on spectra analysis of current and instantaneous power signals," Przeglad Elektrotechniczny ISSN 0033-2097, Iss.12b/2012. – pp. 221–224.

DOI: 01.IJEPE.4.3.5